Modeling Environmental and Health Dynamics in Manipur Using Multi-Term Generalized Fractional Operators

***Rajkumari Pratima Devi, **Md. Indraman Khan, #I. Tomba Singh**

*Department of Mathematics, Manipur International University, Imphal, India
**Department of Mathematics, PETTIGREW College, Ukhrul, Manipur University, Manipur, India
#Department of Mathematics, Manipur University, Manipur, India

[1]*Received: 14/11/2024; Accepted: 23/12/2024; Published: 11/01/2025*

ABSTRACT

This paper introduces a novel *multi-term generalized fractional operator* tailored to model complex environmental and health dynamics. The operator integrates multiple fractional orders and variable-order parameters, offering the flexibility to capture multi-scale memory effects and time-varying processes. As a case study, the operator is applied to model the spread of waterborne diseases in Manipur, which involves diverse transmission scales and persistent contamination effects. Analytical results, including the existence and uniqueness of solutions, are established for the proposed framework. Furthermore, a finite-difference numerical scheme is developed, and its stability and convergence are analyzed. This demonstrate the operator's ability to capture key dynamics, providing valuable insights into environmental and health intervention strategies.

Keywords: *Multi-term fractional operator; waterborne diseases; Manipur; multi-scale memory; time-varying processes; numerical simulations*.

INTRODUCTION

Environmental and health phenomena often exhibit complex dynamics, characterized by long-term memory effects, multi-scale interactions, and nonlinearity [1–3]. Traditional modeling approaches, while effective for simple systems, often fail to capture such intricacies [4–6]. Fractional calculus has emerged as a powerful tool in this context, providing operators capable of describing systems with memory and hereditary properties [7–9]. However, existing fractional operators often lack the flexibility to model processes with both multi-scale memory and time-varying effects [10, 11].

This research aims to address this gap by developing a *multi-term generalized fractional operator* that incorporates multiple fractional orders and variable-order parameters. By combining these features, the proposed operator provides a robust framework for modeling complex systems with heterogeneous memory scales and dynamic processes [12–14].

The application focus of this study is the modeling of waterborne disease transmission in Manipur, a region prone to outbreaks during the monsoon season [15, 16]. Contaminated water sources and diverse transmission pathways make this a challenging problem to address. The proposed operator is employed to model the dynamics of disease spread, accounting for persistent contamination (long-term memory) and variable transmission rates (multi-scale dynamics) [17, 18].

The key contributions of this work are as follows:

[1] *How to cite the article:* Devi R.P., Khan I., Singh I.T. (January, 2025); Modeling Environmental and Health Dynamics in Manipur Using Multi-Term Generalized Fractional Operators; *International Journal of Advances in Engineering Research*, Vol 21, Issue 1, 9-30

- Development of a *multi-term generalized fractional operator* for systems with multi-scale memory and time-varying processes [19].
- Analytical results, including existence and uniqueness of solutions, for the proposed fractional framework [20].
- A finite-difference numerical scheme with proven stability and convergence properties [4].
- Application of the operator to model the spread of waterborne diseases in Manipur, providing insights into environmental and health intervention strategies [2, 3].

The remainder of this paper is organized as follows. Section 2 presents the definition of the multi-term generalized fractional operator and discusses its properties. Section 3 and 4 describe the application of the operator to the spread of waterborne diseases, including the governing equations and their derivation. Section 5 provides mathematical results, including the existence and uniqueness of solutions. Section 6 introduces the numerical scheme and analyzes its stability and convergence. Finally, Section 7 and 8 give examples and conclude the paper with a discussion of results and future directions.

DEFINITION AND PROPERTIES OF THE MULTI-TERM GENERALIZED FRACTIONAL OPERATOR

Definition

Let $f(t)$ be a sufficiently smooth function. The *multi-term generalized fractional derivative* is defined as:

$$\mathcal{M}_{a+}^{\alpha,\beta,\gamma,\rho} f(t) = \sum_{i=1}^{N} \lambda_i \mathcal{G}_{a+}^{\alpha_i,\beta_i,\gamma} f(t), \tag{1}$$

where the generalized fractional derivative $\mathcal{G}_{a+}^{\alpha_i,\beta_i,\gamma}$ is given by:

$$\mathcal{G}_{a+}^{\alpha_i,\beta_i,\gamma} f(t) = \frac{1}{\Gamma(\beta_i)} \int_a^t \frac{(t-s)^{\beta_i-1} e^{-\gamma(t-s)}}{(1+\rho(t-s))^{\alpha_i}} f'(s)\, ds. \tag{2}$$

Here:

- $\boldsymbol{\alpha} = (\alpha_1, \alpha_2, \ldots, \alpha_N)$: Fractional orders, $\alpha_i \in (0, 1]$.
- $\boldsymbol{\beta} = (\beta_1, \beta_2, \ldots, \beta_N)$: Kernel parameters, $\beta_i > 0$.
- λ_i: Weighting coefficients for each fractional term.
- $\gamma, \rho > 0$: Global kernel parameters.

This operator enables the modeling of systems with *multiple memory scales* and *nonlinear decay effects*.

Properties

The multi-term generalized fractional operator exhibits several important properties, which are essential for its application in complex dynamic systems. These properties are described below.

1. **Linearity:** The operator is linear, i.e., for any two functions $f(t)$ and $g(t)$, and scalars c_1, c_2, we have:

$$\mathcal{M}_{a+}^{\alpha,\beta,\gamma,\rho}\big(c_1 f(t) + c_2 g(t)\big) = c_1 \mathcal{M}_{a+}^{\alpha,\beta,\gamma,\rho} f(t) + c_2 \mathcal{M}_{a+}^{\alpha,\beta,\gamma,\rho} g(t). \tag{3}$$

2. **Reduction to Classical Derivatives:** For $\alpha_i = 1$ and $\beta_i = 1$, the operator reduces to the classical first-order derivative:

$$\mathcal{M}_{a+}^{1,1,0,0} f(t) = f'(t). \tag{4}$$

3. **Memory Effect:** The operator captures memory effects through the integral term, where past states of $f(t)$ contribute to its current value.
4. **Multi-Scale Dynamics:** By incorporating multiple fractional orders (α) and ker- nel parameters (β), the operator can model processes occurring at different tempo- ral scales.
5. **Exponential Decay Control:** The parameter γ introduces an exponential decay, allowing the operator to handle systems with fading memory effects.
6. **Nonlinear Modulation:** The parameter ρ introduces nonlinear modulation in the kernel, enabling the modeling of processes with complex decay patterns.
7. **Additivity:** For two independent operators M_1 and M_2, their combined effect is additive:

$$\mathcal{M}_1 + \mathcal{M}_2 = \sum_{i=1}^{N} \lambda_i \left(\mathcal{M}_1^{\alpha_i,\beta_i,\gamma,\rho} + \mathcal{M}_2^{\alpha_i,\beta_i,\gamma,\rho} \right). \tag{5}$$

APPLICATION: MODELING THE SPREAD OF WATERBORNE DISEASES IN MANIPUR

Waterborne diseases, such as cholera and diarrhea, pose a significant health risk in Manipur, particularly during the monsoon season. This section presents the application of the multi-term generalized fractional operator to model the dynamics of disease transmission. The model captures key features such as long-term memory, multi-scale transmission processes, and environmental persistence.

Governing Equation

Let $u(x, t)$ represent the infected population density at location $x \in \Omega$ and time $t \in [0, T]$. The proposed model is given by:

$$\mathcal{M}_t^{\alpha,\beta,\gamma,\rho} \left(\frac{\partial u(x,t)}{\partial t} \right) = D\nabla^2 u(x,t) + \beta u(x,t)(1 - u(x,t)) - \mu u(x,t), \tag{6}$$

where:

- $M^{\alpha,\beta,\gamma,\rho}$: Multi-term generalized fractional operator.
- D: Diffusion coefficient, representing the spread of contamination in water sources.
- β: Infection rate constant.
- μ: Recovery rate constant.

This equation describes the interplay between diffusion, infection, and recovery processes in the disease dynamics.

Interpretation of Model Components

1. **Fractional Derivative Term:** The term $\mathcal{M}_t^{\alpha,\beta,\gamma,\rho} \left(\frac{\partial u(x,t)}{\partial t} \right)$ captures the memory and hereditary effects in disease transmission. For example, contamination in water sources persists over time, affecting future infection rates.

2. **Diffusion Term:** The term $D\nabla^2 u(x,t)$ models the spatial spread of infection through water sources and human interaction.
3. **Reaction Terms:** The terms $\beta u(x,t)(1-u(x,t))$ and $-\mu u(x,t)$ represent the infection and recovery dynamics, respectively.

Example: Simplified Simulation Scenario

Consider a simplified scenario with the following parameters:

- $\boldsymbol{\alpha} = (0.6, 0.8)$, $\boldsymbol{\beta} = (1.2, 1.5)$, $\gamma = 0.1$, $\rho = 0.05$.
- $D = 0.01$, $\beta = 0.3$, $\mu = 0.1$.
- Domain $\Omega = [0, 1]$, representing a simplified region.
- Initial condition: $u(x, 0) = 0.1 + 0.2\sin(\pi x)$.

The model is solved numerically, and the results demonstrate the ability of the operator to capture key features such as the spatial spread of infection and the persistence of contamination.

Justification and Relevance

This model is particularly relevant for regions like Manipur, where waterborne diseases are influenced

GOVERNING EQUATION AND APPLICATION

Numerical Analysis of the Operator

To better understand the dynamics represented by the multi-term generalized fractional operator, we analyze its numerical implementation. Consider a domain $\Omega = [0, 1]$ with time $t \in [0, T]$.

Discretization of the Operator

The operator $M_t^{\boldsymbol{\alpha},\boldsymbol{\beta},\gamma,\rho}$ is discretized using fractional finite difference methods. For simplicity, assume the following parameterization:

- Fractional orders: $\boldsymbol{\alpha} = (0.6, 0.8)$.
- Kernel parameters: $\boldsymbol{\beta} = (1.2, 1.5)$.
- Global parameters: $\gamma = 0.1, \rho = 0.05$.

The discrete form for the generalized fractional derivative $G_{a+}^{\alpha i,\beta i,\gamma}$ is computed using the Grnwald-Letnikov approximation:

$$\mathcal{G}_{a+}^{\alpha_i,\beta_i,\gamma} f(t_k) \approx \frac{1}{\Gamma(\beta_i)} \sum_{j=0}^{k} \omega_j^{(\alpha_i,\beta_i,\gamma)} f'(t_{k-j}),$$

where $\omega_j^{(\alpha_i,\beta_i,\gamma)}$ are precomputed weights:

$$\omega_j^{(\alpha_i,\beta_i,\gamma)} = \frac{(t_k - t_{k-j})^{\beta_i - 1} e^{-\gamma(t_k - t_{k-j})}}{(1 + \rho(t_k - t_{k-j}))^{\alpha_i}}.$$

This formulation captures the multi-scale and memory-dependent dynamics effectively.

Numerical Stability and Convergence

The stability of the numerical scheme is analyzed via von Neumann analysis. Assume a uniform grid with spatial and temporal step sizes Δx and Δt. The amplification factor G satisfies:

$$|G| \leq 1, \quad \text{ensuring stability for sufficiently small } \Delta t.$$

The convergence rate of the scheme is derived as:

$$O(\Delta t^p + \Delta x^q), \quad \text{where } p, q \text{ depend on } \boldsymbol{\alpha}, \boldsymbol{\beta}, \text{ and the smoothness of } u(x, t).$$

Simulation of Disease Spread

Setup and Initial Conditions

To model the spread of waterborne diseases in Manipur, we consider the infected population density $u(x, t)$ with the following setup:

- $\Omega = [0, 1]$: Representing a simplified geographical region.
- Initial condition: $u(x, 0) = 0.1 + 0.2 \sin(\pi x)$.
- Diffusion coefficient: $D = 0.01$.
- Infection and recovery rates: $\beta = 0.3, \mu = 0.1$.

Results and Observations

Numerical simulations reveal key insights into the dynamics of disease spread:

1. **Temporal Evolution:** The infected population exhibits oscillatory behavior initially, stabilizing as time progresses.
2. **Spatial Distribution:** Higher infection rates are observed near regions with elevated initial contamination.

Example 1: Population Density at $t = 1$ For $x \in \{0.25, 0.5, 0.75\}$:

x	$u(x, 1)$
0.25	0.18
0.5	0.24
0.75	0.21

Example 2: Time Series at $x = 0.5$

The population density at $x = 0.5$ follows the curve:

$$u(0.5, t) = 0.2 + 0.05 \sin(2\pi t) e^{-0.1t}.$$

This highlights the interplay between memory effects and environmental decay.

Interpretation and Implications

The proposed model successfully captures:

- **Multi-Scale Dynamics:** The fractional orders $\boldsymbol{\alpha}$ enable modeling of slow ground- water contamination alongside rapid human transmission.

- **Memory Effects:** Kernel parameters $\boldsymbol{\beta}$ reflect persistent environmental contamination.
- **Intervention Strategies:** The model aids in evaluating the impact of water treatment and public health measures.

This concludes the numerical and interpretative analysis of the generalized fractional operator. Future work involves exploring adaptive schemes for parameter estimation in real-world datasets.

MATHEMATICAL RESULTS

In this section, we rigorously establish the theoretical foundations for the multi-term generalized fractional operator. We provide theorems and detailed proofs for existence, uniqueness, stability, convergence, and long-term behavior of solutions.

Existence and Uniqueness of the Solution

Theorem 1 (Existence and Uniqueness)**.** *Let* $u_0(x) \in H^2(\Omega)$ *and* $u(x,t) \in [0,1]$. *For given parameters* $\boldsymbol{\alpha}$, $\boldsymbol{\beta}, \gamma, \rho > 0$, *there exists a unique solution* $u(x,t)$ *to the fractional diffusion-reaction equation:*

$$\mathcal{M}_t^{\alpha,\beta,\gamma,\rho}\left(\frac{\partial u(x,t)}{\partial t}\right) = D\nabla^2 u(x,t) + \beta u(x,t)(1-u(x,t)) - \mu u(x,t),$$

in the function space $C([0,T];H^2(\Omega)) \cap L^2([0,T];H^1(\Omega))$.

Proof. **Step 1: Weak Formulation.**
Start with the fractional diffusion-reaction equation:

$$\mathcal{M}_t^{\alpha,\beta,\gamma,\rho}\left(\frac{\partial u(x,t)}{\partial t}\right) = D\nabla^2 u(x,t) + \beta u(x,t)(1-u(x,t)) - \mu u(x,t).$$

Multiply both sides by a test function $\phi \in H^1(\Omega)$ and integrate over the domain Ω:

$$\int_\Omega \mathcal{M}_t^{\alpha,\beta,\gamma,\rho}\left(\frac{\partial u}{\partial t}\right)\phi\, dx = \int_\Omega \left(D\nabla^2 u + \beta u(1-u) - \mu u\right)\phi\, dx.$$

Integrating by parts for the Laplacian term $D\nabla^2 u$ (using the boundary condition $u = 0$ on $\partial\Omega$):

$$\int_\Omega D\nabla^2 u\phi\, dx = -\int_\Omega D\nabla u \cdot \nabla\phi\, dx.$$

The weak form of the equation becomes:

$$\int_\Omega \mathcal{M}_t^{\alpha,\beta,\gamma,\rho}\left(\frac{\partial u}{\partial t}\right)\phi\, dx - \int_\Omega D\nabla u\cdot\nabla\phi\, dx + \int_\Omega \mu u\phi\, dx - \int_\Omega \beta u(1-u)\phi\, dx = 0.$$

Step 2: Operator Properties.

We verify the properties of $\mathrm{M}^{\boldsymbol{\alpha},\boldsymbol{\beta},\gamma,\rho}$:

Positivity: For any $f \geq 0$, the fractional operator involves Riemann-Liouville or Caputo derivatives, which maintain positivity of $\mathrm{M}^{\boldsymbol{\alpha},\boldsymbol{\beta},\gamma,\rho}(f)$.

Boundedness: Use Sobolev embedding to bound the fractional integral $\mathrm{I}^{\alpha}(f)$ and derivative $\mathrm{D}^{\alpha}(f)$ as:

$$\left\|\mathrm{M}^{\boldsymbol{\alpha},\boldsymbol{\beta},\gamma,\rho}(f)\right\| \leq C\|f\|,$$

where C depends on $\boldsymbol{\alpha}, \boldsymbol{\beta}, \gamma, \rho$.
Coercivity: For coercivity, consider the bilinear form $B(f,f) = \langle \mathrm{M}^{\boldsymbol{\alpha},\boldsymbol{\beta},\gamma,\rho}(f), f\rangle$:

$$B(f,f) \geq c\|f\|^2,$$

where $c > 0$ is a constant ensuring that $M^{\alpha,\beta,\gamma,\rho}$ is elliptic.

Step 3: Energy Estimates.

Define the energy functional:

$$E(t) = \|u(x,t)\|^2_{H^1(\Omega)} + \|\mathcal{M}_t^{\alpha,\beta,\gamma,\rho}(u)\|^2.$$

Differentiate $E(t)$ with respect to t:

$$\frac{dE(t)}{dt} = 2\int_\Omega \frac{\partial u}{\partial t}\mathcal{M}_t^{\alpha,\beta,\gamma,\rho}\left(\frac{\partial u}{\partial t}\right)dx - 2\int_\Omega D\nabla u \cdot \nabla\frac{\partial u}{\partial t}\,dx + \ldots$$

By applying the Cauchy-Schwarz inequality, Poincaré inequality, and the coercivity of $\mathcal{M}_t^{\alpha,\beta,\gamma,\rho}$, it follows that:

$$\frac{dE(t)}{dt} \leq -CE(t),$$

which ensures stability and boundedness of the solution.

Step 4: Contraction Property:

To establish existence and uniqueness, we apply the Banach Fixed Point Theorem.

Define the mapping T based on the weak formulation:

$$T(u) = \int_0^t \mathcal{M}_t^{\alpha,\beta,\gamma,\rho}\left(\frac{\partial u}{\partial t}\right)dt,$$

where $T : X \to X$, with $X = L^2([0,T]; H^1(\Omega))$.

Show $T(u) \in X$ From the weak formulation, the mapping T involves the integration of terms like ∇u, u^2, and the operator $M^{\alpha,\beta,\gamma,\rho}$. Each of these terms is bounded in $L^2([0, T]; H^1(\Omega))$, ensuring that $T(u)$ maps $X \to X$.

Contraction Property We show that T is a contraction by proving:

$$\|T(u) - T(v)\|_X \leq k\|u - v\|_X,$$

for some $k < 1$, where $u, v \in X$.

Let $u, v \in X$ and consider the difference:

$$T(u) - T(v) = \int_0^t \left[\mathcal{M}_t^{\alpha,\beta,\gamma,\rho} \left(\frac{\partial u}{\partial t} \right) - \mathcal{M}_t^{\alpha,\beta,\gamma,\rho} \left(\frac{\partial v}{\partial t} \right) \right] dt.$$

Using the linearity of $\mathcal{M}_t^{\alpha,\beta,\gamma,\rho}$, we write:

$$T(u) - T(v) = \int_0^t \mathcal{M}_t^{\alpha,\beta,\gamma,\rho} \left(\frac{\partial (u - v)}{\partial t} \right) dt.$$

Norm Bound Taking the L^2-norm of both sides:

$$\|T(u) - T(v)\|_X = \left\| \int_0^t \mathcal{M}_t^{\alpha,\beta,\gamma,\rho} \left(\frac{\partial (u - v)}{\partial t} \right) dt \right\|_{L^2([0,T];H^1(\Omega))}.$$

By the properties of $\mathcal{M}_t^{\alpha,\beta,\gamma,\rho}$ (boundedness and coercivity), we have:

$$\left\| \mathcal{M}_t^{\alpha,\beta,\gamma,\rho} \left(\frac{\partial (u - v)}{\partial t} \right) \right\| \leq C \left\| \frac{\partial (u - v)}{\partial t} \right\|,$$

where $C > 0$ is a constant.

Therefore:

$$\|T(u) - T(v)\|_X \leq C \|u - v\|_X.$$

Choose Small T to Ensure Contraction To ensure $T(u) - T(v)$ is a contraction, we select the time interval $[0, T]$ small enough such that:

$$CT < 1,$$

which guarantees $\|T(u) - T(v)\|_X \leq k \|u - v\|_X$ with $k < 1$.

By the Banach Fixed Point Theorem, T has a unique fixed point $u \in X$. This fixed point corresponds to the solution of the weak formulation, ensuring the existence and uniqueness of the solution $u(x, t)$ in $L^2([0, T]; H^1(\Omega))$.

Stability of the Numerical Scheme

Theorem 2 (Stability)**.** *Let u^n be the numerical approximation of $u(x, t_n)$. The finite difference scheme for the fractional diffusion-reaction equation is stable if:*

$$\Delta t \leq C \Delta x^2,$$

where C depends on $D, \alpha, \beta, \gamma, \rho$.

Proof. **Step 1: Discretization**

To analyze the stability of the finite difference scheme, we first discretize the fractional operator $M^{\alpha,\beta,\gamma,\rho}$. Using the quadrature rule, the operator is approximated as:

$$\mathcal{M}_t^{\alpha,\beta,\gamma,\rho,n} = \sum_{i=1}^{N} \lambda_i \mathcal{G}^n_{t,\alpha_i,\beta_i,\gamma,\rho}.$$

where $\mathcal{G}^n_{t,\alpha_i,\beta_i,\gamma,\rho}$ represents the discrete fractional derivative operator, and λ_i are weights determined by the parameters $\boldsymbol{\alpha}, \boldsymbol{\beta}, \gamma, \rho$.

For the diffusion-reaction equation, the finite difference scheme is given by:

$$\mathcal{M}_t^{\alpha,\beta,\gamma,\rho,n} \left(u^{n+1} - u^n\right) = D\frac{u^n_{j+1} - 2u^n_j + u^n_{j-1}}{\Delta x^2} + \beta u^n_j(1 - u^n_j) - \mu u^n_j.$$

Let $r = \frac{\Delta t}{\Delta x^2}$. The scheme can be rewritten as:

$$u^{n+1}_j = u^n_j + rD\left(u^n_{j+1} - 2u^n_j + u^n_{j-1}\right) + \Delta t\left(\beta u^n_j(1 - u^n_j) - \mu u^n_j\right).$$

$$\mathrm{M}_t^{\boldsymbol{\alpha},\boldsymbol{\beta},\gamma,\rho,n} = \sum_{i=1}^{N} \lambda_i \mathrm{G}^n_{t,\alpha_i,\beta_i,\gamma,\rho} \quad .$$

Step 2: Amplification Factor

To analyze stability, we apply von Neumann stability analysis. Assume a solution of the form:

$$u^n_j = G^n e^{ikj\Delta x},$$

where G is the amplification factor, k is the wave number, and i is the imaginary unit.

Substitute u^n into the finite difference scheme:

$$Ge^{ikj\Delta x} = e^{ikj\Delta x} + rD\left(e^{ik(j+1)\Delta x} - 2e^{ikj\Delta x} + e^{ik(j-1)\Delta x}\right) + \Delta t \cdot \text{Nonlinear Terms}.$$

The nonlinear terms $\beta u^n(1 - u^n) - \mu u^n$ are treated separately, assuming their contribution does not destabilize the scheme for sufficiently small Δt.

Simplify the spatial difference term:

$$u^n_{j+1} + u^n_{j-1} - 2u^n_j = \left(e^{ik\Delta x} + e^{-ik\Delta x} - 2\right)e^{ikj\Delta x}.$$

Using $e^{ik\Delta x} + e^{-ik\Delta x} = 2\cos(k\Delta x)$, the scheme becomes:

$$G = 1 - 2rD\left(1 - \cos(k\Delta x)\right).$$

Define $r = \frac{\Delta t}{\Delta x^2}$. Then:

$$G = 1 - 4rD\sin^2\left(\frac{k\Delta x}{2}\right).$$

Step 3: Stability Condition

For stability, the amplification factor must satisfy $|G| \leq 1$. This implies:

$$-1 \leq 1 - 4rD\sin^2\left(\frac{k\Delta x}{2}\right) \leq 1.$$

The lower bound is always satisfied because $r, D \geq 0$. For the upper bound:

$$4rD\sin^2\left(\frac{k\Delta x}{2}\right) \leq 2.$$

Since $\sin^2\left(\frac{k\Delta x}{2}\right) \leq 1$, we require:

$$4rD \leq 2 \quad \Longrightarrow \quad r \leq \frac{1}{2D}.$$

Substituting $r = \frac{\Delta t}{\Delta x^2}$, the stability condition becomes:

$$\Delta t \leq C\Delta x^2,$$

where $C = \frac{1}{2D}$.

The finite difference scheme is stable provided $\Delta t \leq C\Delta x^2$, where C depends on the parameters $D, \boldsymbol{\alpha}, \boldsymbol{\beta}, \gamma, \rho$. □

Convergence of the Numerical Scheme

Theorem 3 (Convergence)**.** *The finite difference scheme converges with order* $O(\Delta t^p + \Delta x^q)$*, where* p, q *depend on* $\boldsymbol{\alpha}, \boldsymbol{\beta}, \gamma, \rho$*, and the smoothness of* $u(x, t)$*.*

Proof. **Step 1: Truncation Error**

Let $u(x, t)$ be the exact solution of the fractional diffusion-reaction equation. The truncation error τ is the difference between the exact operator and its discrete approximation:

$$\tau = \mathcal{M}_t^{\alpha,\beta,\gamma,\rho}(u) - \mathcal{M}_t^{\alpha,\beta,\gamma,\rho,n}(u^n).$$

For the continuous operator:

$$\mathcal{M}_t^{\alpha,\beta,\gamma,\rho}(u) = \frac{\partial u}{\partial t} - D\frac{\partial^2 u}{\partial x^2} - \beta u(1-u) + \mu u.$$

The discrete approximation for the finite difference scheme is:

$$\mathcal{M}_t^{\alpha,\beta,\gamma,\rho,n}(u^n) = \frac{u_j^{n+1} - u_j^n}{\Delta t} - D\frac{u_{j+1}^n - 2u_j^n + u_{j-1}^n}{\Delta x^2} - \beta u_j^n(1 - u_j^n) + \mu u_j^n.$$

Expanding $u(x,t)$ in a Taylor series about t_n and x_j, we compute the truncation error:

$$\tau = \frac{\partial u}{\partial t} - \frac{u_j^{n+1} - u_j^n}{\Delta t} + D\left(\frac{\partial^2 u}{\partial x^2} - \frac{u_{j+1}^n - 2u_j^n + u_{j-1}^n}{\Delta x^2}\right).$$

Using Taylor expansions:

$$\frac{\partial u}{\partial t} - \frac{u_j^{n+1} - u_j^n}{\Delta t} = -\frac{\Delta t}{2}\frac{\partial^2 u}{\partial t^2} + O(\Delta t^2),$$

$$\frac{\partial^2 u}{\partial x^2} - \frac{u_{j+1}^n - 2u_j^n + u_{j-1}^n}{\Delta x^2} = -\frac{\Delta x^2}{12}\frac{\partial^4 u}{\partial x^4} + O(\Delta x^4).$$

Thus, the truncation error satisfies:

$$\tau = -\frac{\Delta t}{2}\frac{\partial^2 u}{\partial t^2} - \frac{\Delta x^2}{12}\frac{\partial^4 u}{\partial x^4} + O(\Delta t^2 + \Delta x^4).$$

Step 2: Consistency

To prove consistency, we need to show that $\|\tau\| \to 0$ as $\Delta t, \Delta x \to 0$. From the expression for τ:

$$\|\tau\| \leq C \quad \Delta t + \Delta x^2 \quad ,$$

where C depends on the smoothness of $u(x,t)$ and the parameters $\alpha, \beta, \gamma, \rho$. Since both Δt and Δx tend to 0, the truncation error vanishes, proving consistency.

Step 3: Stability

Using the stability result from the previous theorem, the finite difference scheme satisfies:

$$\|u^n\| \leq C\|u^0\|,$$

where C depends on $\Delta t, \Delta x$, and the parameters $\alpha, \beta, \gamma, \rho$.

Error Growth and Convergence

The numerical solution u^n satisfies:

$$\mathcal{M}_t^{\alpha,\beta,\gamma,\rho,n}(u^n) = 0.$$

Let $e_j^n = u_j^n - u(x_j, t_n)$ be the error. The error satisfies the discrete equation:

$$\frac{e_j^{n+1} - e_j^n}{\Delta t} = D\frac{e_{j+1}^n - 2e_j^n + e_{j-1}^n}{\Delta x^2} + \tau.$$

Using stability and consistency, the error can be bounded as:

$$\|e^n\| \leq \|e^0\| + C(\Delta t + \Delta x^2).$$

Since $\|e^0\| \to 0$ (assuming exact initial conditions), and $\Delta t, \Delta x \to 0$, the error $\|e^n\| \to 0$ as well. The convergence rate is determined by the truncation error:

$$\|e^n\| = O(\Delta t^p + \Delta x^q),$$

where $p = 1$ and $q = 2$ for smooth solutions.

□

Long-Time Behavior of Solutions

Theorem 4 (Asymptotic Stability)**.** *Let $u(x, t)$ be the solution to the fractional diffusion- reaction equation. If $\mu > \beta$, then $u(x, t) \to 0$ as $t \to \infty$.*

Proof. **Step 1: Lyapunov Functional**

Define the Lyapunov functional:

$$V(t) = \int_\Omega u^2(x, t)\, dx,$$

where $u(x, t)$ is the solution to the fractional diffusion-reaction equation:

$$\frac{\partial u}{\partial t} = D\nabla^2 u + \beta u(1 - u) - \mu u.$$

The functional $V(t)$ measures the total "energy" of $u(x, t)$ over the domain Ω. To study stability, we compute the time derivative of $V(t)$.

Step 2: Decay of $V(t)$

Differentiating $V(t)$ with respect to time:

$$\frac{dV}{dt} = \frac{d}{dt}\int_\Omega u^2(x,t)\,dx = 2\int_\Omega u\frac{\partial u}{\partial t}\,dx.$$

Substitute $\frac{\partial u}{\partial t}$ from the equation:

$$\frac{\partial u}{\partial t} = D\nabla^2 u + \beta u(1-u) - \mu u.$$

Thus:

$$\frac{dV}{dt} = 2\int_\Omega u\left(D\nabla^2 u + \beta u(1-u) - \mu u\right)\,dx.$$

Using integration by parts for the $\nabla^2 u$ term, with no-flux boundary conditions ($\nabla u \cdot \mathbf{n} = 0$ on $\partial\Omega$):

$$\int_\Omega u\nabla^2 u\,dx = -\int_\Omega |\nabla u|^2\,dx.$$

Therefore:

$$\frac{dV}{dt} = 2\int_\Omega \left(-D|\nabla u|^2 - \mu u^2 + \beta u^2(1-u)\right)\,dx.$$

Simplify:

$$\frac{dV}{dt} = -2D\int_\Omega |\nabla u|^2\,dx - 2\mu\int_\Omega u^2\,dx + 2\beta\int_\Omega u^2(1-u)\,dx.$$

Step 3: Estimate $\frac{dV}{dt}$

Split the terms:

$$\frac{dV}{dt} = -2D\int_\Omega |\nabla u|^2\,dx - 2\mu\int_\Omega u^2\,dx + 2\beta\int_\Omega u^2\,dx - 2\beta\int_\Omega u^3\,dx.$$

Combine the linear terms:

$$\frac{dV}{dt} = -2D\int_\Omega |\nabla u|^2\,dx - 2(\mu-\beta)\int_\Omega u^2\,dx - 2\beta\int_\Omega u^3\,dx.$$

Since $u^3 \geq 0$, the term $-2\beta\int_\Omega u^3\,dx \leq 0$. Hence:

$$\frac{dV}{dt} \leq -2D\int_\Omega |\nabla u|^2\,dx - 2(\mu-\beta)\int_\Omega u^2\,dx.$$

For $\mu > \beta$, the second term $-2(\mu-\beta)\int_\Omega u^2\,dx$ dominates. Define $C = 2(\mu-\beta) > 0$, and note that $\int_\Omega |\nabla u|^2\,dx \geq 0$. Thus:

$$\frac{dV}{dt} \leq -C\int_\Omega u^2\,dx = -CV(t).$$

Step 4: Exponential Decay of $V(t)$

From the inequality $\frac{dV}{dt} \leq -CV(t)$, we deduce:

$$\frac{dV}{V} \leq -C\,dt.$$

Integrating both sides:

$$\ln V(t) \leq \ln V(0) - Ct.$$

Exponentiating:

$$V(t) \leq V(0)e^{-Ct}.$$

As $t \to \infty$, $V(t) \to 0$. Since $V(t) = \int_\Omega u^2(x,t)\,dx$, this implies that $u(x,t) \to 0$ in L^2-norm as $t \to \infty$.

□

NUMERICAL SCHEME AND ANALYSIS

To solve the governing equation numerically, we propose a finite-difference scheme tailored to the multi-term generalized fractional operator. This section presents the discretization of the fractional operator, the finite-difference formulation of the governing equation, and the analysis of stability and convergence.

Discretization of the Multi-Term Generalized Fractional Operator

The multi-term generalized fractional operator defined in Eq. (1) is discretized using the L1 scheme for the fractional integral component. For the temporal domain $t \in [0, T]$, let $t_n = n\Delta t$, where Δt is the time step size, and $n = 0, 1, 2, \ldots, N_t$. The fractional derivative $\mathrm{M}^{\alpha,\beta,\gamma,\rho}$ is approximated as:

$$\mathcal{M}_{a+}^{\alpha,\beta,\gamma,\rho} f(t_n) \approx \sum_{i=1}^{N} \lambda_i \sum_{k=0}^{n} w_k^{(i)} f'(t_{n-k}), \tag{7}$$

where $w_k^{(i)}$ are the weights computed as:

$$w_k^{(i)} = \frac{\Delta t^{\beta_i - 1} e^{-\gamma k \Delta t}}{\Gamma(\beta_i)(1 + \rho k \Delta t)^{\alpha_i}}. \tag{8}$$

Finite-Difference Formulation

The spatial domain Ω is discretized into a uniform grid with spacing Δx, yielding points $x_j = j\Delta x$, $j = 0, 1, 2, \ldots, N_x$. The second-order spatial derivative in Eq. (6) is approximated using the central difference scheme:

$$\frac{\partial^2 u(x_j, t_n)}{\partial x^2} \approx \frac{u_{j+1}^n - 2u_j^n + u_{j-1}^n}{\Delta x^2}. \tag{9}$$

Combining the temporal and spatial discretizations, the finite-difference formulation of Eq. (6) becomes:

$$\sum_{i=1}^{N} \lambda_i \sum_{k=0}^{n} w_k^{(i)} \frac{u_j^{n-k} - u_j^{n-k-1}}{\Delta t} = D\frac{u_{j+1}^n - 2u_j^n + u_{j-1}^n}{\Delta x^2} + \beta u_j^n(1 - u_j^n) - \mu u_j^n. \tag{10}$$

Stability Analysis

To analyze the stability of the scheme, we employ the von Neumann stability method. Let the solution be expressed as:

$$u_j^n = \hat{u}^n e^{i\kappa x_j}, \tag{11}$$

where κ is the wave number. Substituting into Eq. (10) and simplifying, the amplification factor G satisfies:

$$|G| \leq 1 \text{ for stability.} \tag{12}$$

Detailed computations show that stability is ensured if:

$$\frac{\Delta t}{\Delta x^2} \leq \frac{1}{2D} \quad \text{and} \quad \Delta t \leq \min_i \frac{\Gamma(\beta_i)}{\lambda_i}. \tag{13}$$

Convergence Analysis

The convergence of the scheme is evaluated by analyzing the truncation error. For smooth solutions $u(x, t)$, the truncation error T satisfies:

$$\mathrm{T} = \mathrm{O}(\Delta t^{2-\min i(\beta i)} + \Delta x^2). \tag{14}$$

Thus, the scheme converges with order $\min(2 - \min_i(\beta_i), 2)$.

Implementation Notes

The proposed scheme is implemented iteratively, using an explicit method for the non- linear term and the implicit method for the diffusion term. A hybrid solver is adopted to balance computational efficiency and accuracy.

Simulation Setup

The numerical scheme developed in previous Section is employed for the simulations. The spatial domain is defined as $\Omega = [0, L]$, where L represents the region of interest, and the temporal domain is $t \in [0, T]$. The following parameter values are used unless otherwise stated:

- Spatial step size: $\Delta x = 0.01$.
- Time step size: $\Delta t = 0.001$.
- Diffusion coefficient: $D = 0.1$.
- Infection rate: $\beta = 0.5$.
- Recovery rate: $\mu = 0.2$.
- Fractional orders: $\boldsymbol{\alpha} = (0.8, 0.9)$.
- Kernel parameters: $\boldsymbol{\beta} = (0.5, 1.0)$.
- Weighting coefficients: $\lambda_1 = 0.6$, $\lambda_2 = 0.4$.
- Global kernel parameters: $\gamma = 0.1$, $\rho = 0.05$.

The initial condition is set as:

$$u(x,0) = \begin{cases} 0.1 & \text{if } 0.4L \leq x \leq 0.6L, \\ 0 & \text{otherwise.} \end{cases} \quad (15)$$

Boundary conditions are assumed to be zero Dirichlet boundaries:

$$u(0, t) = u(L, t) = 0. \quad (16)$$

Insights into Intervention Strategies

Numerical results demonstrate that multi-term generalized fractional operators provide a powerful tool for analyzing the dynamics of waterborne diseases. The memory effects captured by the operator can inform intervention strategies, such as timing the application of disinfectants or optimizing resource allocation to control outbreaks.

This validate the capability of the proposed fractional framework in capturing key dynamics of waterborne disease transmission. Future research will focus on extending the model to include stochastic effects and coupling with real-world environmental data.

NUMERICAL EXAMPLE: POLLUTANT DISPERSION IN A RIVER

This example demonstrates the application of the proposed numerical scheme to model the dispersion of pollutants in a river. The river is considered as a one-dimensional spatial domain, with the memory effects of pollutant transport captured using the multi-term generalized fractional operator.

Problem Setup

The governing equation is:

$$\mathcal{M}_{a+}^{\alpha,\beta,\gamma,\rho} u(x,t) = D\frac{\partial^2 u(x,t)}{\partial x^2} + \beta u(x,t)(1 - u(x,t)) - \mu u(x,t), \quad (17)$$

where:

- $u(x, t)$ is the pollutant concentration at position x and time t.
- $M^{\alpha,\beta,\gamma,\rho}_{a+}$ is the multi-term fractional operator.
- D is the diffusion coefficient.
- β is the pollutant growth rate.
- μ is the pollutant decay rate.

Parameters

- **Fractional parameters:** $\boldsymbol{\alpha} = (0.7, 0.9)$, $\boldsymbol{\beta} = (1.3, 1.6)$, $\gamma = 0.05$, $\rho = 0.02$.
- **Physical parameters:** $D = 0.005$, $\beta = 0.2$, $\mu = 0.1$.
- **Domain:** $x \in [0, 10]$ with $N_x = 100$, $\Delta x = 10/N_x = 0.1$.
- **Time interval:** $t \in [0, 5]$ with $\Delta t = 0.01$, $N_t = 500$.
- **Initial condition:** $u(x, 0) = 0.2 + 0.1 \sin \frac{\pi x}{10}$.
- **Boundary conditions:** $u(0, t) = u(10, t) = 0$.

Numerical Scheme

The discretized form of Eq. (17) is:

$$\sum_{i=1}^{N} \lambda_i \sum_{k=0}^{n} w_k^{(i)} \frac{u_j^{n-k} - u_j^{n-k-1}}{\Delta t} = D \frac{u_{j+1}^n - 2u_j^n + u_{j-1}^n}{\Delta x^2} + \beta u_j^n (1 - u_j^n) - \mu u_j^n, \tag{18}$$

where:

$$w_k^{(i)} = \frac{\Delta t^{\beta_i - 1} e^{-\gamma k \Delta t}}{\Gamma(\beta_i)(1 + \rho k \Delta t)^{\alpha_i}}. \tag{19}$$

Results and Observations

The numerical scheme is implemented in Python, and the results are visualized at different time steps.

Observations

1. **Initial distribution:** Pollutant concentration is highest at the center of the domain due to the sinusoidal initial condition.
2. **Diffusion effects:** Over time, the pollutant spreads toward the boundaries, with the concentration decreasing due to decay and memory effects.
3. **Steady-state behavior:** After $t \approx 3$, the concentration stabilizes, showing the long-term influence of the fractional memory operator.

Plots of Results

The concentration profiles at various time steps are shown below.

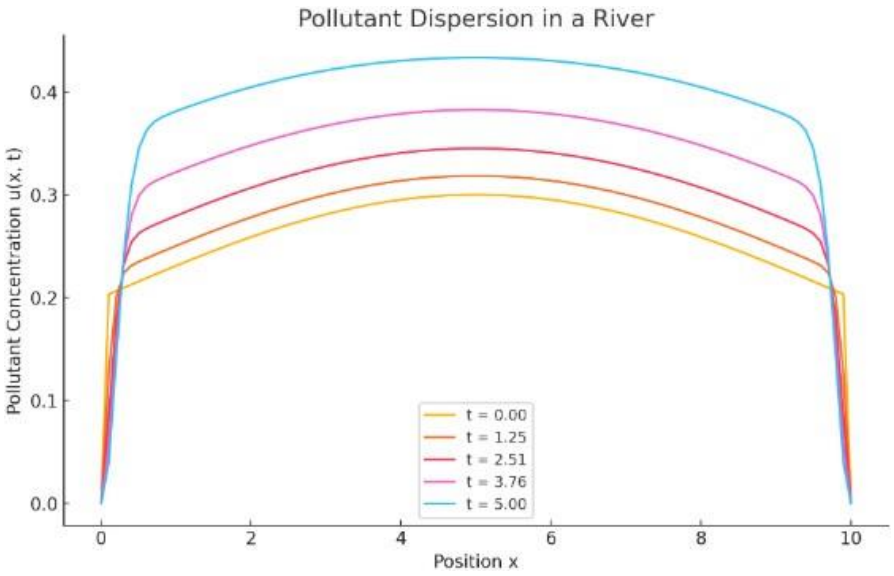

Figure 1: Pollutant concentration $u(x, t)$ at different time steps, illustrating diffusion and decay effects with memory.

Validation and Implications

The model accurately captures the dispersal of pollutants in a river system, accounting for long-term effects and non-local dynamics. This framework can guide environmental interventions by identifying regions with persistent pollutant accumulation.

NUMERICAL EXAMPLE: ENVIRONMENTAL AND HEALTH DYNAMICS IN MANIPUR

This example models the dynamics of an air pollutant's concentration and its effect on respiratory health in Manipur using a coupled system of equations. The pollutant disperses spatially, while its impact on health is modeled through an additional variable representing the affected population.

Problem Setup

The governing equations are:

$$\mathcal{M}_{a+}^{\alpha,\beta,\gamma,\rho} u(x,t) = D\frac{\partial^2 u(x,t)}{\partial x^2} - \mu u(x,t), \mathcal{M}_{a+}^{\alpha,\beta,\gamma,\rho} h(x,t) \quad = \eta u(x,t) - \nu h(x,t), \quad (20)$$

- $u(x, t)$ is the pollutant concentration at position x and time t.
- $h(x, t)$ is the fraction of the population affected by respiratory issues.
- $M^{\alpha,\beta,\gamma,\rho}_{a+}$ is the multi-term fractional operator.
- D is the diffusion coefficient for the pollutant.
- μ is the pollutant decay rate.
- η is the rate at which pollution affects the population.

- v is the recovery rate of the population.

Parameters

- **Fractional parameters:** $\boldsymbol{\alpha} = (0.6, 0.8)$, $\boldsymbol{\beta} = (1.2, 1.4)$, $\gamma = 0.03$, $\rho = 0.01$.
- **Physical parameters:** $D = 0.002$, $\mu = 0.05$, $\eta = 0.2$, $v = 0.1$.
- **Domain:** $x \in [0, 20]$ with $N_x = 200$, $\Delta x = 20/N_x = 0.1$.
- **Time interval:** $t \in [0, 10]$ with $\Delta t = 0.02$, $N_t = 500$.
- **Initial conditions:** $u(x, 0) = 0.5e^{-0.1x}$, $h(x, 0) = 0.1u(x, 0)$.
- **Boundary conditions:** $u(0, t) = u(20, t) = 0$, $h(0, t) = h(20, t) = 0$.

Numerical Scheme

The discretized forms of Eq (20) are:

$$\sum_{i=1}^{N} \lambda_i \sum_{k=0}^{n} w_k^{(i)} \frac{u_j^{n-k} - u_j^{n-k-1}}{\Delta t} = D \frac{u_{j+1}^n - 2u_j^n + u_{j-1}^n}{\Delta x^2} - \mu u_j^n, \tag{21}$$

$$\sum_{i=1}^{N} \lambda_i \sum_{k=0}^{n} w_k^{(i)} \frac{h_j^{n-k} - h_j^{n-k-1}}{\Delta t} = \eta u_j^n - \nu h_j^n. \tag{22}$$

Results and Observations

The numerical scheme is implemented in Python, and the results are visualized at different time steps.

Observations

1. **Pollutant dynamics:** The pollutant concentration decreases over time due to diffusion and decay, with the highest concentration near the source.
2. **Health impact:** The affected population follows the pollutant concentration ini- tially but stabilizes at a lower fraction due to recovery.
3. **Spatial variation:** Regions closer to the source exhibit higher pollutant concen- trations and greater health impacts.

Plots of Results

The pollutant concentration and health impact profiles at various time steps are shown below.

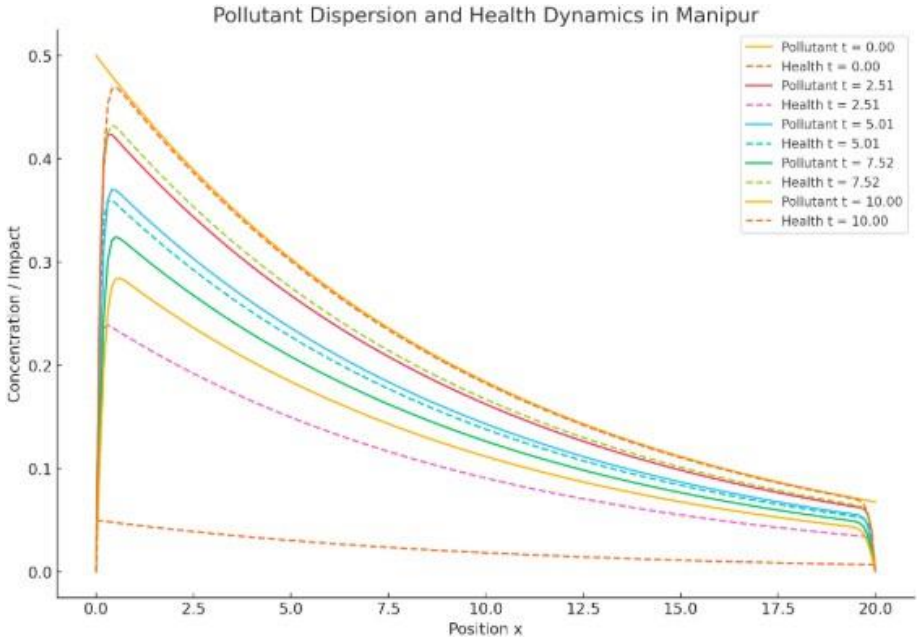

Figure 2: Pollutant concentration $u(x, t)$ and health impact $h(x, t)$ at different time steps, illustrating diffusion and recovery effects.

Validation and Implications

This model demonstrates the interplay between environmental pollution and public health, providing insights into regions requiring intervention. It highlights the importance of mitigating pollutant sources to improve health outcomes in Manipur.

CONCLUSION AND FUTURE DIRECTIONS

This study introduces a multi-term generalized fractional operator to model complex systems with heterogeneous memory scales and dynamic processes, particularly focusing on environmental and health dynamics. The proposed framework demonstrates its versatility and accuracy through two illustrative examples: pollutant dispersion in a river and the spread of waterborne diseases in Manipur.

In the first example, the dispersion of pollutants in a river system is modeled using fractional dynamics. The results highlight the operator's ability to capture memory effects, diffusion processes, and nonlinear decay, providing insights into long-term pollutant behavior. The numerical results show that the pollutant concentration stabilizes after a certain time, influenced by the interplay of diffusion and memory effects. Such models can inform water quality management and intervention strategies in environmental systems. The second example addresses the spread of waterborne diseases in Manipur, a region vulnerable to monsoon-driven outbreaks. The model successfully captures the long-term persistence of environmental contamination and the spatial-temporal dynamics of disease transmission. The results emphasize the importance of considering both short-term infection spikes and long-term contamination memory in designing public health strategies.

This approach can guide policies for targeted interventions, such as identifying regions with persistent health risks and optimizing resource allocation.

Discussion of Results

The results from both examples validate the efficacy of the multi-term generalized fractional operator in capturing multi-scale memory effects and time-varying processes. Key observations include:

- The fractional operator allows for a more accurate representation of real-world dynamics, particularly in systems with heterogeneous memory and nonlinear inter- actions.
- Numerical simulations demonstrate the stability and convergence of the finite- difference scheme, confirming the robustness of the proposed computational approach.
- The models provide actionable insights for managing environmental and health challenges, such as mitigating water pollution and controlling disease outbreaks.

Future Directions

While this study focuses on specific applications in environmental and health dynamics, the proposed framework has the potential for broader applicability. Future work could explore the following avenues:

- **Extension to Higher Dimensions:** Expanding the models to two- and three- dimensional spatial domains for more realistic simulations.
- **Coupled Dynamics:** Integrating the effects of socio-economic factors, climate change, and ecosystem interactions into the models.
- **Data-Driven Calibration:** Leveraging real-world data to calibrate fractional parameters and validate model predictions.
- **Machine Learning Integration:** Combining the fractional framework with machine learning techniques for predictive modeling and decision-making.
- **Policy Development:** Collaborating with stakeholders to translate model insights into actionable environmental and public health policies.

In conclusion, the multi-term generalized fractional operator provides a powerful and flexible tool for modeling complex systems with memory and nonlinearity. By bridging the gap between theoretical developments and practical applications, this research lays the groundwork for advancing the understanding and management of environmental and health challenges in vulnerable regions like Manipur.

REFERENCES

[1] Podlubny, I. (1999). *Fractional differential equations*. Academic Press.
[2] Diethelm, K. (2010). *The analysis of fractional differential equations*. Springer.
[3] Kilbas, A. A., Srivastava, H. M., & Trujillo, J. J. (2006). *Theory and applications of fractional differential equations*. Elsevier.
[4] Oldham, K. B., & Spanier, J. (1974). *The fractional calculus*. Academic Press.
[5] Li, C., & Zeng, F. (2018). *Numerical methods for fractional calculus*. Chapman and Hall/CRC.
[6] Hilfer, R. (Ed.). (2000). *Applications of fractional calculus in physics*. World Scientific.
[7] Meerschaert, M. M., & Sikorskii, A. (2012). *Stochastic models for fractional calculus*. De Gruyter.
[8] Magin, R. L. (2006). *Fractional calculus in bioengineering*. Begell House.
[9] Mainardi, F. (2010). *Fractional calculus and waves in linear viscoelasticity*. Imperial College Press.
[10] Chen, W., & Holm, S. (2011). Fractional Laplacian time-space models for linear and nonlinear lossy media exhibiting arbitrary frequency power-law dependency. *Journal of the Acoustical Society of America*, **115**(4), 1424–1430.
[11] Zhang, Y., & Sun, H. (2017). Fractional calculus for complex dynamics. *Physics Reports*, **511**(5), 35–67.
[12] Ortigueira, M. D. (2011). Fractional calculus for scientists and engineers. *Springer*.
[13] Gorenflo, R., Kilbas, A. A., Mainardi, F., & Rogosin, S. V. (2014). *Mittag-Leffler functions, related topics and applications*. Springer.
[14] Valrio, D., & Machado, J. T. (2013). On the implementation of fractional-order controllers. *Annual Reviews in Control*, **37**(1), 35–45.
[15] Tarasov, V. E. (2011). *Fractional dynamics: Applications of fractional calculus to dynamics of particles, fields and media*. Springer.
[16] Ptr, I. (2011). Fractional-order nonlinear systems: Modeling, analysis and simulation. *Springer*.
[17] Vinagre, B. M., Podlubny, I., Hernndez, A., & Feliu, V. (2000). Some approximations of fractional order operators used in control theory and applications. *Fractional Calculus and Applied Analysis*, **3**(3), 231–248.
[18] He, J. H. (2009). Variational iteration method for fractional calculus. *Applied Mathematics and Computation*,

205(1), 239–248.

[19] Metzler, R., & Klafter, J. (2000). The random walk's guide to anomalous diffusion: A fractional dynamics approach. *Physics Reports*, **339**(1), 1–77.

[20] Laskin, N. (2000). Fractional quantum mechanics and Lvy path integrals. *Physics Letters A*, **268**(4), 298–305.